



## Article

# Single Ionization of He by Energetic Protons in a Parabolic Quasi-Sturmians Approach

Sergey A. Zaytsev <sup>1,\*</sup>, Alexander S. Zaytsev <sup>1,†</sup>, Vyacheslav V. Nasyrov <sup>1,†</sup>, Darya S. Zaytseva <sup>1,†</sup>, Lorenzo U. Ancarani <sup>2,†</sup> and Konstantin A. Kouzakov <sup>3,†</sup>

<sup>1</sup> School of Fundamental and Computer Sciences, Pacific National University, 680035 Khabarovsk, Russia; AlZaytsev@pnu.edu.ru (A.S.Z.); VVNasyrov@pnu.edu.ru (V.V.N.); 2012002939@pnu.edu.ru (D.S.Z.)

<sup>2</sup> Laboratory of Physics and Theoretic Chemistry, National Center for Scientific Research, Lorraine University, 57000 Metz, France; ugo.ancarani@univ-lorraine.fr

<sup>3</sup> Department of Nuclear Physics and Quantum Theory of Collisions, Faculty of Physics, Lomonosov Moscow State University, 119991 Moscow, Russia; kouzakov@gmail.com

\* Correspondence: zaytsevs@pnu.edu.ru

† These authors contributed equally to this work.

**Abstract:** A fully differential cross section for single ionization of helium induced by 1 MeV proton impact is calculated using the parabolic convoluted quasi-Sturmian (CQS) method. In the framework of this approach the transition amplitude is extracted directly from the asymptotic behavior of the solution of an inhomogeneous Schrödinger equation for the Coulomb three-body system ( $e^-$ ,  $\text{He}^+$ ,  $p^+$ ). The driven equation is solved numerically by expanding in convolutions of quasi-Sturmians for the two-body proton- $\text{He}^+$  and electron- $\text{He}^+$  systems. It is found, at least in the high energy limit, that the calculated cross sections within the proposed CQS method converge quickly as the number of terms in the expansions is increased, and are in reasonable agreement with experimental data and other theoretical results.

**Keywords:** ionization by proton impact; parabolic coordinates; Green's function; quasi-Sturmian; asymptotic behavior



**Citation:** Zaytsev, S.A.; Zaytsev, A.S.; Nasyrov, V.V.; Zaytseva, D.S.; Ancarani, L.U.; Kouzakov, K.A. Single Ionization of He by Energetic Protons in a Parabolic Quasi-Sturmians Approach. *Atoms* **2022**, *10*, 13. <https://doi.org/10.3390/atoms10010013>

Academic Editor: Yew Kam Ho

Received: 30 December 2021

Accepted: 22 January 2022

Published: 25 January 2022

**Publisher's Note:** MDPI stays neutral with regard to jurisdictional claims in published maps and institutional affiliations.



**Copyright:** © 2022 by the authors. Licensee MDPI, Basel, Switzerland. This article is an open access article distributed under the terms and conditions of the Creative Commons Attribution (CC BY) license (<https://creativecommons.org/licenses/by/4.0/>).

## 1. Introduction

Recently, the fully differential cross sections (FDCSs) of singly ionizing 1-MeV  $p^+ + \text{He}$  collisions in various kinematical regimes characterized by momentum-transfer values  $q \lesssim 2$  a.u. and ejected-electron energy  $E_e \lesssim 20$  eV, have been measured with high precision [1,2] using cold target recoil ion momentum spectroscopy (COLTRIMS) [3–5]. The data analysis clearly revealed insufficiencies of the first Born approximation (FBA). For this reason, more advanced approaches have been tested. The well-known continuum-distorted-wave eikonal initial state (CDW-EIS) model [6,7] and its variations have been applied to the calculation of FDCSs [8–10]. Another semiclassical approach called the wave-packet convergent close-coupling (WP-CCC) method [11,12] has also been used. Within this method the electronic part of the wave function in a combined potential of the projectile and target (in the framework of the frozen-core approximation) is expanded in terms of bound states and wave-packet pseudostates describing the active electron of the helium atom; these wave-packet pseudostates represent a finite interval of the active electron continuum. Along with the semiclassical approaches, fully quantum mechanical treatments beyond FBA have also been considered. In Refs. [2,13], FDCSs were calculated using the 3C model [14,15] which takes into account paired Coulomb interactions between the final charged fragments ( $p^+$ ,  $e^-$ ,  $\text{He}^+$ ) by means of the corresponding Coulomb wave functions with, in general, effective charges.

Despite the considerable theoretical effort, none of the approaches have been able to completely explain the experimental observations. The measured ejected-electron angular distribution in the scattering plane and the corresponding theoretical calculations present

a usual two-peak structure: a large (named binary) and a small (named recoil) peak separated by minima of almost zero intensity. The FBA predicts the binary peak to be located exactly in the momentum transfer direction and the recoil peak in its opposite direction. However, in the experimental data both peaks are shifted towards the forward direction. The theoretical approaches that go beyond the FBA explain the shift only partly but clearly fail to give a proper account of the experimentally observed features of the binary peak. This failure clearly calls for further development of our theoretical understanding of ion–atom ionizing collisions.

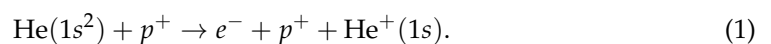
In this work we propose and apply a novel quantum approach, based on convoluted quasi-Sturmian functions, and named CQS, that accounts for the total energy spectrum of the active electron. In order to satisfy properly the boundary conditions involving the plane wave of high-energy protons, it is convenient to use parabolic coordinates with the axis  $\hat{z}$  chosen along the incident proton momentum  $\mathbf{K}_0$ . Within the frozen-core approximation, we consider an inhomogeneous Schrödinger equation for the Coulomb three-body system  $(e^-, \text{He}^+, p^+)$ , in which the driven term contains the incident channel interaction. The driven equation is solved with an expansion in convolutions of quasi-Sturmians for the  $(e^-, \text{He}^+)$  and  $(\text{He}^+, p^+)$  subsystems. An auxiliary proton plane wave (with a momentum  $Q \lesssim K_0$ ) is introduced into the basis functions in order to avoid numerical evaluations of integrals with very rapidly oscillating integrands. Within the proposed approach the Coulomb  $p - e$  interaction is treated as a perturbation and approximated by a truncated basis of square integrable ( $L^2$ ) Sturmian functions in parabolic coordinates. Making use of asymptotic properties of the CQS basis functions, the transition amplitude is extracted directly from the asymptotic behavior of the solution, without the need of calculating a six-dimensional matrix element.

The plan of the paper is as follows. In Section 2.1, in the framework of the frozen-core approximation, a driven equation is formulated, whose solution’s asymptotic behavior is directly related to the transition amplitude. In Section 2.2, we give the parabolic quasi-Sturmian functions over which the solution is expanded (Section 2.3). Making use of the analytically known asymptotic properties of the basis functions, we express the transition amplitude in terms of *basis amplitudes*. In Section 2.4, we describe the matrix equation method allowing one to obtain the coefficients of the expansion. Specifically, the matrix equation is obtained from the driven equation by using finite Sturmian-expansion representations of the  $p - e$  interaction and Green’s function of the two non-interacting subsystems  $(e^-, \text{He}^+)$  and  $(\text{He}^+, p^+)$ . In Section 3, after providing some details of our FDCSs calculations, we make a comparison with the experimental data and theoretical cross sections obtained by other authors. A summary is presented in Section 4.

Atomic units are used throughout unless otherwise specified.

## 2. The CQS Approach

We outline, here, the convoluted quasi-Sturmian (CQS) treatment (more details will be provided in [16]) of the ionization process



### 2.1. Amplitude

In the framework of the frozen-core model the amplitude is cast in the form

$$T_{\mathbf{K}, \mathbf{k}_e} = \langle \Psi_{\mathbf{K}, \mathbf{k}_e}^{(-)}, \psi_{1s}^{\text{He}^+} | \hat{V} | \mathbf{K}_0, \Phi^{(0)} \rangle. \tag{2}$$

Here the final state  $\Psi_{\mathbf{K}, \mathbf{k}_e}^{(-)}$  is a solution to the Schrödinger equation

$$[E - \hat{H}] | \Psi_{\mathbf{K}, \mathbf{k}_e}^{(-)} \rangle = 0, \tag{3}$$

for the three-body system  $(e^-, He^+, p^+) = (1, 2, 3)$ , where  $\mathbf{k}_e$  denotes the momentum of the ejected electron while  $\mathbf{K}$  is the momentum of the scattered proton (we assume that the helium nucleus is at rest during the process). The energy of the system is given by  $E = \frac{k_e^2}{2} + \frac{K^2}{2m_p}$ . We define the electron and proton relative coordinates as

$$\begin{aligned} \mathbf{r} &= \mathbf{r}_1 - \mathbf{r}_2, \\ \mathbf{R} &= \mathbf{r}_3 - \mathbf{r}_2, \end{aligned} \tag{4}$$

and denote by  $(\theta_e, \phi_e)$  and  $(\theta_p, \phi_p)$  the respective polar and azimuthal angles. The initial state  $|\mathbf{K}_0, \Phi^{(0)}\rangle$  is represented by the product of a helium ground state  $\Phi^{(0)}(\mathbf{r}, \mathbf{r}')$  and the plane wave

$$\langle \mathbf{R} | \mathbf{K}_0 \rangle = e^{i\mathbf{K}_0 \cdot \mathbf{R}} \tag{5}$$

describing the incident proton, whereas  $\hat{V}$  is the incident channel interaction

$$V(\mathbf{R}, \mathbf{r}) = \frac{1}{R} - \frac{1}{|\mathbf{R} - \mathbf{r}|}. \tag{6}$$

The amplitude, symmetrized in the coordinates  $\mathbf{r}$  and  $\mathbf{r}'$ , of the electrons is:

$$T_{\mathbf{K}, \mathbf{k}_e}^S = \sqrt{2} \langle \Psi_{\mathbf{K}, \mathbf{k}_e}^{(-)} | \hat{V} | \mathbf{K}_0, f \rangle, \tag{7}$$

where

$$f(\mathbf{r}) = \int \psi_{1s}^{He^+}(\mathbf{r}') \Phi^{(0)}(\mathbf{r}, \mathbf{r}') d^3 r'. \tag{8}$$

Let us apply the three-body Green function  $\hat{G}^{(+)}(E) \equiv [E - \hat{H}]^{-1}$  corresponding to Equation (3) to the vector  $\hat{V} | \mathbf{K}_0, f \rangle$ . Since the latter vanishes sufficiently rapidly for large values of the hyperradius  $\rho = \sqrt{m_p R^2 + r^2}$ , the final state  $\Psi_{\mathbf{K}, \mathbf{k}_e}^{(-)}(\mathbf{R}, \mathbf{r})$  appears in the leading asymptotic form of [17,18]

$$\begin{aligned} \langle \mathbf{R}, \mathbf{r} | \hat{G}^{(+)} \hat{V} | \mathbf{K}_0, f \rangle &\simeq \frac{m_p}{(2\pi)^2} \frac{(2E)^{3/4} e^{i\frac{\pi}{4}}}{(2\pi)^{1/2}} \\ &\times \frac{\exp\{i[\sqrt{2E}\rho + W_0(\mathbf{R}, \mathbf{r})]\}}{\rho^{5/2}} \langle \Psi_{\mathbf{K}, \mathbf{k}_e}^{(-)} | \hat{V} | \mathbf{K}_0, f \rangle, \end{aligned} \tag{9}$$

where  $W_0$  is the Coulomb phase [17]

$$W_0(\mathbf{R}, \mathbf{r}) = -\frac{\rho}{\sqrt{2E}} \left( \frac{1}{R} - \frac{1}{r} - \frac{1}{|\mathbf{R} - \mathbf{r}|} \right) \ln(2\sqrt{2E}\rho). \tag{10}$$

Here the  $\hat{\mathbf{K}}$  and  $\hat{\mathbf{k}}_e$  directions are those of  $\hat{\mathbf{R}}$  and  $\hat{\mathbf{r}}$ , respectively, while the ratio  $K/k_e$  is determined by the hyperangle  $\gamma$

$$\tan \gamma = \frac{r}{\sqrt{m_p} R}, \tag{11}$$

namely

$$K = \sqrt{2E} \cos(\gamma), \quad k_e = \sqrt{2E} \sin(\gamma). \tag{12}$$

Thus, the problem of determining the transition amplitude can be cast in the form of the inhomogeneous equation

$$[E - \hat{H}] | \Phi^{(+)} \rangle = \hat{V} | \mathbf{K}_0, f \rangle \tag{13}$$

with outgoing boundary conditions, whose asymptotic behavior contains the sought-for amplitude.

### 2.2. Parabolic Quasi-Sturmians

To properly account for the high-energy incident proton, we set the problem in parabolic coordinates with the  $\hat{z}$ -axis defined by the direction of the incident proton momentum  $\mathbf{K}_0$ . Specifically, we suggest solving the driven Equation (13) numerically using an expansion

$$|\Phi^{(+)}\rangle = \sum_{\mathfrak{N}} C_{\mathfrak{N}} |\mathcal{S}_{\mathbf{Q},\mathfrak{N}}^{(+)}\rangle, \tag{14}$$

in terms of the so-called parabolic shifted quasi-Sturmians that satisfy the equation

$$[E - \hat{H}_0] |\mathcal{S}_{\mathbf{Q},\mathfrak{N}}^{(+)}\rangle = |\mathbf{Q}, \tilde{\mathfrak{N}}\rangle, \tag{15}$$

where  $\hat{H}_0$  is the Hamiltonian

$$\hat{H}_0 = -\frac{1}{2m_p} \nabla_{\mathbf{R}}^2 - \frac{1}{2} \nabla_{\mathbf{r}}^2 + \frac{1}{R} - \frac{1}{r}. \tag{16}$$

In analogy with the driven Equation (13), we have introduced into the right-hand side of (15) an auxiliary proton plane wave with the momentum  $\mathbf{Q} = \varepsilon \mathbf{K}_0$ ,  $\varepsilon < 1$ . Its purpose will be explained in Section 3. The symbol  $\mathfrak{N}$  denotes the labels  $\{n_1, n_2, m_1, m_2, \varkappa\}$  of products of basis Sturmian functions [19]:

$$|\mathfrak{N}\rangle \equiv |n_1, n_2, \varkappa\rangle |m_1, m_2, -\varkappa\rangle, \tag{17}$$

of the parabolic coordinates  $\xi_1, \eta_1, \phi_1$  and  $\xi_2, \eta_2, \phi_2$  associated with  $\mathbf{R}$  and  $\mathbf{r}$ , respectively. Specifically,

$$\langle \xi, \eta, \phi | n_1, n_2, \varkappa \rangle = \frac{e^{i\varkappa\phi}}{\sqrt{2\pi}} \varphi_{n_1}^{|\varkappa|}(\xi) \varphi_{n_2}^{|\varkappa|}(\eta), \tag{18}$$

where the square-integrable functions  $\varphi_n^\lambda$ ,  $\lambda = |\varkappa|$ , are defined in terms of the associated Laguerre polynomials  $L_n^\lambda$  [20],

$$\varphi_n^\lambda(x) = \sqrt{\frac{2bn!}{(n+\lambda)!}} (2bx)^{\lambda/2} e^{-bx} L_n^\lambda(2bx) \tag{19}$$

with the basis scale parameter  $b$ . In turn,  $|\tilde{\mathfrak{N}}\rangle$  represents the orthogonal complement to (17):

$$|\tilde{\mathfrak{N}}\rangle \equiv |\widetilde{n_1, n_2, \varkappa}\rangle |m_1, m_2, -\varkappa\rangle, \tag{20}$$

where

$$|\widetilde{n, m, \varkappa}\rangle = w |n, m, \varkappa\rangle, \quad w(\xi, \eta) = \frac{4}{\xi + \eta}, \tag{21}$$

so that

$$\langle \widetilde{n, m, \varkappa} | n', m', \varkappa' \rangle = \delta_{n,n'} \delta_{m,m'} \delta_{\varkappa,\varkappa'} \quad \text{and} \quad \langle \tilde{\mathfrak{N}} | \mathfrak{N}' \rangle = \delta_{\mathfrak{N},\mathfrak{N}'}. \tag{22}$$

### 2.3. Basis Amplitudes

Formally, the quasi-Sturmians  $|\mathcal{S}_{\mathbf{Q},\mathfrak{N}}^{(+)}\rangle$  are expressed as a convolution of the two quasi-Sturmians [19]:

$$|\mathcal{S}_{\mathbf{Q},\mathfrak{n}}^{p(+)}\rangle = \hat{G}_0^{p(+)} \left( \frac{p^2}{2m_p} \right) |\mathbf{Q}\rangle |\widetilde{n_1, n_2, \varkappa}\rangle, \quad \mathfrak{n} \equiv \{n_1, n_2, \varkappa\}, \tag{23}$$

and

$$|\mathcal{S}_{\mathfrak{m}}^{e(+)}\rangle = \hat{G}_0^{e(+)} \left( \frac{k^2}{2} \right) |m_1, m_2, -\varkappa\rangle, \quad \mathfrak{m} \equiv \{m_1, m_2, \varkappa\}, \tag{24}$$

where  $\hat{G}_0^{p(+)}$  and  $\hat{G}_0^{e(+)}$  are the two-body Green's functions for the proton and electron moving in the Coulomb field of the ion, with, respectively, Sommerfeld parameters  $\beta_p = \frac{m_p}{P}$  and  $\beta_e = -\frac{1}{k}$ . On the other hand, Equation (15) is equivalent to

$$|\mathcal{S}_{\mathbf{Q},\mathfrak{M}}^{(+)}\rangle = \hat{G}_0^{(+)}(E)|\mathbf{Q},\mathfrak{M}\rangle, \tag{25}$$

where  $\hat{G}_0^{(+)}(E) \equiv [E - \hat{H}_0]^{-1}$  is the three-body Green's function associated with  $\hat{H}_0$ . Thus, the asymptotic behavior of  $|\mathcal{S}_{\mathbf{Q},\mathfrak{M}}^{(+)}\rangle$  can be obtained from that of  $\hat{G}_0^{(+)}$  [17]. Specifically, we may use its representation in the form of a convolution integral (see, e.g., [21,22])

$$\hat{G}_0^{(+)}(E) = \frac{1}{2\pi i} \int_{\mathcal{C}} d\mathcal{E} \hat{G}_0^{e(+)}(\mathcal{E}) \hat{G}_0^{p(+)}(E - \mathcal{E}), \tag{26}$$

where the contour  $\mathcal{C}$  runs just above the unitary cut and bound-state poles of  $\hat{G}_0^{e(+)}$  (see Figure 1).

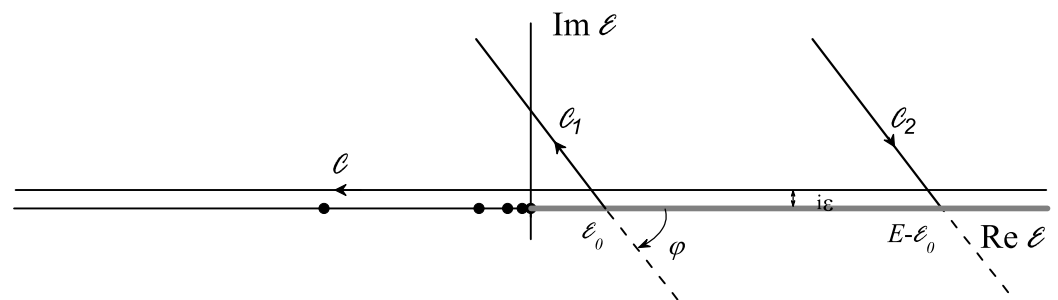


**Figure 1.** The path of integration of the convolution integral is the whole real  $\mathcal{E}$  axis, from  $\infty$  to  $-\infty$ . The gray line is the unitarity branch cut for  $\hat{G}_0^{e(+)}$ . The path  $\mathcal{C}_1$  is obtained by a negative angle  $\varphi$  rotation of  $\mathcal{C}$ , about some point  $\mathcal{E}_0$  on the positive real axis. The argument of  $\hat{G}_0^{p(+)}$  therewith follows the path  $\mathcal{C}_2$ .

The integration can be performed with the method of stationary phase (see, e.g., [17]), and one finds

$$\begin{aligned} \langle \mathbf{R}, \mathbf{r} | \mathcal{S}_{\mathbf{Q},\mathfrak{M}}^{(+)} \rangle &\simeq m_p \frac{(2E)^{3/4} e^{i\frac{\pi}{4}}}{(2\pi)^{1/2}} \\ &\times \frac{\exp\{i[\sqrt{2E}\rho - \beta_p \ln(2\sqrt{2E}\rho(\cos\gamma)^2) - \beta_e \ln(2\sqrt{2E}\rho(\sin\gamma)^2)]\}}{\rho^{5/2}} \\ &\times \frac{e^{i\pi(\phi_p - \phi_e)}}{2\pi} \mathcal{A}_n^{p(+)}(K, Q; \theta_p) \mathcal{A}_m^{e(+)}(k_e; \theta_e). \end{aligned} \tag{27}$$

The amplitudes  $\mathcal{A}_m^{e(+)}$  and  $\mathcal{A}_n^{p(+)}$ , derived by analytical techniques developed in [19] and whose lengthy mathematical derivation is to be found in [16], are given by

$$\begin{aligned} \mathcal{A}_m^{e(+)}(k; \theta_e) &= \frac{i}{k} \sqrt{\frac{m_1! m_2!}{(m_1 + \lambda)! (m_2 + \lambda)!}} \zeta^{-i\beta_e} e^{-\frac{\pi\beta_e}{2}} \left(\frac{1}{\zeta} - \zeta\right)^{\lambda+1} \left(\frac{\sin\theta_e}{2}\right)^\lambda \\ &\times (-\zeta)^{m_1+m_2} \sum_{\nu_1=0}^{m_1} \sum_{\nu_2=0}^{m_2} c_{\nu_1}^{(m_1,\lambda)} c_{\nu_2}^{(m_2,\lambda)} \Gamma(i\beta_e + \lambda + \nu_1 + \nu_2 + 1) \\ &\times (1 - \zeta^{-2})^{\nu_1+\nu_2} \left(\cos\frac{\theta_e}{2}\right)^{2\nu_1} \left(\sin\frac{\theta_e}{2}\right)^{2\nu_2}, \\ \zeta &= \frac{b + \frac{ik}{2}}{b - \frac{ik}{2}}, \end{aligned} \tag{28}$$

$$\begin{aligned}
 \mathcal{A}_n^{p(+)}(P, Q; \theta_p) &= \frac{i}{P} \sqrt{\frac{n_1!n_2!}{(n_1+\lambda)!(n_2+\lambda)!}} \left[ \frac{1+(p+q)}{1-(p-q)} \frac{1}{c^2+\alpha s^2} \right]^{i\beta_p} e^{-\frac{\pi\beta_p}{2}} \\
 &\times \left[ \frac{4p}{1-(p-q)^2} \frac{1}{c^2+\alpha s^2} \right]^{1+\lambda} \left( \frac{\sin \theta_p}{2} \right)^\lambda \left[ -\frac{1-(p+q)}{1+(p+q)} \right]^{n_1} \left[ -\frac{1-(p-q)}{1+(p-q)} \right]^{n_2} \\
 &\times \sum_{\mu_1=0}^{n_1} \sum_{\mu_2=0}^{n_2} c_{\mu_1}^{(n_1,\lambda)} c_{\mu_2}^{(n_2,\lambda)} \Gamma(i\beta_p + \lambda + \mu_1 + \mu_2 + 1) \\
 &\times \left[ \frac{-4p}{[1-(p+q)][1-(p-q)]} \frac{1}{c^2+\alpha s^2} \right]^{\mu_1+\mu_2} (c^2)^{\mu_1} (\alpha s^2)^{\mu_2}, \\
 p &= -\frac{iP}{2b}, \quad q = -\frac{iQ}{2b}, \quad \alpha = \frac{1-(p+q)^2}{1-(p-q)^2}, \\
 c &= \cos \frac{\theta_p}{2}, \quad s = \sin \frac{\theta_p}{2}.
 \end{aligned}
 \tag{29}$$

Here,

$$\lambda = |\varkappa|, \quad c_\nu^{(n,\lambda)} = (-1)^\nu \frac{(n+\lambda)!}{(n-\nu)!(\nu+\lambda)! \nu!}.
 \tag{30}$$

Finally, comparing the asymptotic behavior (9) of the solution  $|\Phi^{(+)}\rangle$  to (13) and that of the quasi-Sturmians (27) we deduce that the transition amplitude  $T_{\mathbf{K},\mathbf{k}_e}$  is expressed up to a phase factor in terms of the coefficients  $C_{\mathfrak{N}}$  of the expansion (14), as

$$T_{\mathbf{K},\mathbf{k}_e}^S = \sqrt{22}\pi \sum_{\mathfrak{N}} C_{\mathfrak{N}} e^{i\varkappa(\phi_p-\phi_e)} \mathcal{A}_n^{p(+)}(K, Q; \theta_p) \mathcal{A}_m^{e(+)}(k_e; \theta_e).
 \tag{31}$$

A remarkable feature of this result is that the angular dependence of the transition amplitude is found only in  $\mathcal{A}_n^{p(+)}$  and  $\mathcal{A}_m^{e(+)}$  that we name *basis amplitudes*.

#### 2.4. Equation for $C_{\mathfrak{N}}$

Let us write the Hamiltonian  $\hat{H}$  in the frozen-core approximation

$$\hat{H} = \hat{H}_0 + \hat{U},
 \tag{32}$$

$$U(\mathbf{R}, \mathbf{r}) = -\frac{1}{|\mathbf{R} - \mathbf{r}|}.
 \tag{33}$$

Using the proposed expansion (14), projecting by  $|\mathbf{Q}, \mathfrak{N}\rangle$  from the left, and inserting the unit operator  $\sum_{\mathfrak{M}} |\mathfrak{M}\rangle \langle \mathfrak{M}|$ , the driven Equation (13) is converted into the following matrix equation

$$\sum_{\mathfrak{N}'} \left[ \delta_{\mathfrak{N},\mathfrak{N}'} - \langle \mathfrak{N} | \hat{U} | \mathfrak{N}' \rangle \langle \mathbf{Q}, \mathfrak{N} | \hat{G}_0^{(+)}(E) | \mathbf{Q}, \mathfrak{N}' \rangle \right] C_{\mathfrak{N}'} = D_{\mathfrak{N}},
 \tag{34}$$

where

$$D_{\mathfrak{N}} \equiv \langle \mathfrak{N} | \hat{V} | \mathbf{K}_0 - \mathbf{Q}, f \rangle.
 \tag{35}$$

Since the Coulomb proton–electron interaction in (33) is treated as a perturbation, the corresponding logarithmic phase factor will not be present in the solution  $|\Phi^{(+)}\rangle$  asymptotic behavior. Nevertheless, we believe that this absence will not substantially affect the cross section, at least in this high-energy case. In our approach the operator  $\hat{U}$  is approximated by the truncated expansion over parabolic Sturmians (17):

$$\begin{aligned}
 \hat{U}^{\mathcal{N}_0} &= \sum_{\varkappa,\varkappa'=-M_0}^{M_0} \sum_{n_1,n_2,m_1,m_2=0}^{N_0-1} \sum_{n'_1,n'_2,m'_1,m'_2=0}^{N_0-1} \\
 &|\widetilde{n_1, n_2, \varkappa}\rangle | \widetilde{m_1, m_2, -\varkappa} \rangle U_{n_1,n_2,m_1,m_2; n'_1,n'_2,m'_1,m'_2}^{\varkappa,\varkappa'} |\widetilde{n'_1, n'_2, \varkappa'}\rangle | \widetilde{m'_1, m'_2, -\varkappa'} \rangle,
 \end{aligned}
 \tag{36}$$

where

$$U_{n_1, n_2, m_1, m_2; n'_1, n'_2, m'_1, m'_2}^{\varkappa, \varkappa'} = \langle n_1, n_2, \varkappa | \langle m_1, m_2, -\varkappa | \hat{U} | n'_1, n'_2, \varkappa' \rangle | m'_1, m'_2, -\varkappa' \rangle. \quad (37)$$

The Green's function operator matrix elements are evaluated numerically by using the contour  $\mathcal{C}_1$  (see Figure 1) [22,23]:

$$\begin{aligned} \langle \mathbf{Q}, \tilde{\mathfrak{N}} | \hat{G}_0^{(+)}(E) | \mathbf{Q}, \tilde{\mathfrak{N}}' \rangle &= \frac{1}{2\pi i} \int_{\mathcal{C}_1} d\mathcal{E} \langle \widetilde{m_1, m_2, -\varkappa} | \hat{G}_0^{e(+)}(\mathcal{E}) | \widetilde{m'_1, m'_2, -\varkappa} \rangle \\ &\times \langle \widetilde{n_1, n_2, \varkappa} | \langle \mathbf{Q} | \hat{G}_0^{p(+)}(E - \mathcal{E}) | \mathbf{Q} \rangle | \widetilde{n'_1, n'_2, \varkappa} \rangle. \end{aligned} \quad (38)$$

Both factors in the integrand are expressed analytically (see, e.g., [19]). Ideally we would put  $\mathbf{Q} = \mathbf{K}_0$  and thereby incorporate the incident proton plane wave into the Green's function matrix element. However, we found out that the correct evaluation of the contour integral (38) requires the condition

$$E - \mathcal{E}_0 > \frac{Q^2}{2m_p}. \quad (39)$$

Note that  $E - \mathcal{E}_0$  is the point of the intersection of the contour  $\mathcal{C}_2$  with the real energy axis (see Figure 1).

The 'external' coefficients  $C_{\mathfrak{N}}$ , whose indices are not involved in the expansion (36), coincide with the corresponding coefficients  $D_{\mathfrak{N}}$  of the expansion of the driven term while the 'internal' coefficients are found as a solution to a finite system (34) with an appropriately modified right-hand side.

### 3. Results and Discussion

We now present results of numerical calculations of FDCS which, in the laboratory frame, reads

$$\frac{d^5\sigma}{dE_e d\Omega_e d\Omega_p} = k_e \frac{m_p^2}{(2\pi)^5} \frac{K}{K_0} \left| T_{\mathbf{K}, \mathbf{k}_e}^S \right|^2. \quad (40)$$

We consider here the ionization in coplanar geometry, and fix the kinematic conditions as follows [1]: the incident proton energy is  $E_p = 1$  MeV, the ejected electron energy is  $E_e = 6.5$  eV, and the momentum transfer is relatively small,  $q = 0.75$  a.u. We will therefore plot the calculated FDCS as a function of the electron scattering angle  $\theta_e$ . These differential cross sections typically feature two peaks: one (binary) peak is close to the direction of the momentum transfer  $\mathbf{q} = \mathbf{K}_0 - \mathbf{K}$  while the other (recoil) peak is close to the opposite direction. In our calculations we have used the ground state wave function  $\Phi^{(0)}$  obtained by diagonalization of the helium Hamiltonian (see, e.g., [24]).

We have examined the convergence behavior of the expansion (31) (with  $C_{\mathfrak{N}}$  equal to  $D_{\mathfrak{N}}$  (35) for  $\mathbf{Q} = \mathbf{K}_0$ ) and thus determined limits  $M$  and  $N$  to the ranges  $|\varkappa| \leq M$  and  $n_j, m_j < N, j = 1, 2$ . Specifically, we have found that satisfactory convergence of the cross section can be achieved with  $N \approx 20$ . Moreover, the value of  $M$  turns out to be limited due to the smallness of the proton scattering angle  $\theta_p$ , so that convergence is observed already at  $M = 3$ . In all calculations, we set the basis (19) scale parameter  $b = 1$ .

The driven Equation (13) is then solved numerically using separable expansions for both  $\hat{U}$  and  $\hat{G}_0^{(+)}$ . The auxiliary proton plane wave  $|\mathbf{Q}\rangle$  has been introduced into the basis functions (23) as to eliminate the rapidly oscillating factor from the right-hand side of Equation (13). For this purpose it would be convenient to put  $Q = K_0$ . On the other hand, numerical computation of the Green's function matrix elements imposes the constraint (39) on  $Q$ . In order to bring  $Q$  as close as possible to  $K_0$ , we should choose the value of  $\mathcal{E}_0 > 0$  as small as possible. In our case, the energy of the incident proton is  $E_p \simeq 36,749.33$ , so that the total energy of the scattered proton and the ejected electron is  $E = E_p + \varepsilon_0^{\text{He}} - \varepsilon_0^{\text{He}^+} \simeq 36,748.42$ . Then putting  $\mathcal{E}_0 = E \times 10^{-5} \simeq 0.36748$  enables us to

choose  $Q = 0.999945K_0$  and get the value 0.63893 for the difference  $K_0 - Q$  which appears when computing the coefficients (35).

Then by considering the matrix Equation (34) for the ‘internal’ coefficients, we have examined the convergence behavior of the transition amplitude (31) as the number of terms in the representation (36) is increased. It has been found that the convergence of the cross section is achieved at  $M_0 = 3$  and  $N_0 = 9$ . (For  $N_0 = 9$  the total number  $\mathcal{N}_0$  of Sturmian functions (17) involved in the potential separable expansion (36) is equal to 45,927.)

We have also considered refining the final channel interaction by replacing the Coulomb potential  $1/R$  for the proton and  $-1/r$  for the electron by, respectively, with the Hartree potentials for the  $(e^-, He^+)$  and  $(p^+, He^+)$  systems. This means that  $\tilde{U}$  (33) is replaced by

$$\tilde{U}(\mathbf{R}, \mathbf{r}) = -\frac{1}{|\mathbf{R}-\mathbf{r}|} - \frac{1}{r} + \left\langle \psi_{1s}^{He^+} \left| \frac{1}{|\mathbf{r}-\mathbf{r}'|} \right| \psi_{1s}^{He^+} \right\rangle + \frac{1}{R} - \left\langle \psi_{1s}^{He^+} \left| \frac{1}{|\mathbf{R}-\mathbf{r}'|} \right| \psi_{1s}^{He^+} \right\rangle. \tag{41}$$

The results of this refinement are shown in Figure 2 in comparison with those corresponding to purely Coulomb potentials. It can be seen that such short-range additions to the Coulomb interactions have little effect on the positions of the cross section’s peaks.

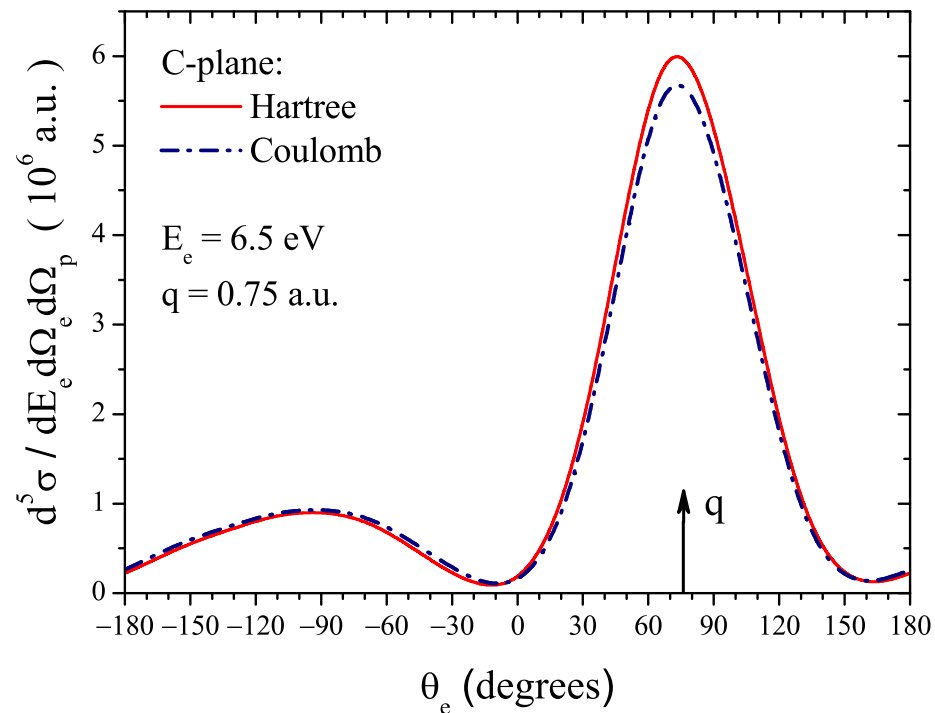


**Figure 2.** FDCS for single ionization of helium by 1-MeV protons in the collision plane. The electron emission energy is  $E_e = 6.5$  eV, and the total momentum transfer  $q = 0.75$  a.u. Solid curve shows the results obtained with the Hartree potentials for the  $(e^-, He^+)$  and  $(p^+, He^+)$  systems. Dash-dotted line corresponds to the case of pure Coulomb interactions. The arrow indicates the direction of the momentum transfer.

In Figure 3 we present a comparison of our laboratory frame cross sections with experimental data and other theoretical calculations. Theoretical values are obtained using our approach, the WP-CCC method [11] (the latter results calculated in the relative coordinate system are multiplied by  $(m_p/\mu)^2 = 25/16$ ), the first Born approximation (FBA) and 3C model [13]. The experimental values are due to Ref. [1] with normalization of Ref. [13].



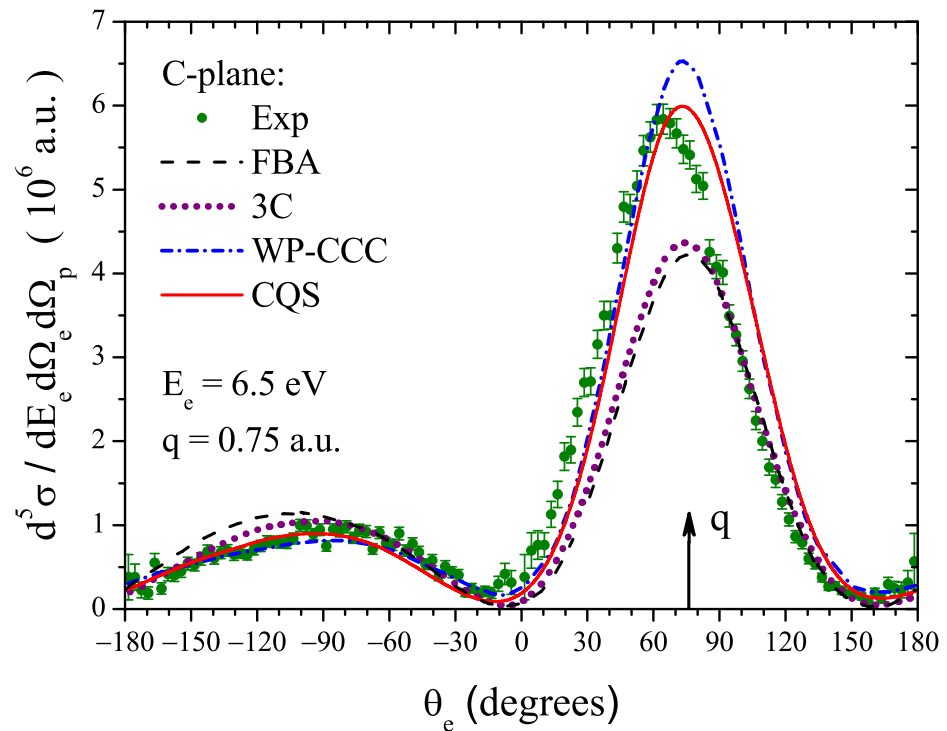


**Figure 3.** FDCS for single ionization of helium by 1-MeV protons in the collision plane. The electron emission energy is  $E_e = 6.5$  eV, and the total momentum transfer  $q = 0.75$  a.u. Solid curve shows the results obtained with our method of convoluted quasi-Sturmians (CQS). Experimental data are shown by filled circles with error bars, the FBA and 3C calculations (using a strongly correlated ground-state wave function of helium [25]) by dashed and dotted lines respectively, and the dash-dotted line represents the WP-CCC results.

Since the WP-CCC calculations were presented in Ref. [11] without convolution and with experimental uncertainties; in order to compare our results and those of other theoretical approaches on equal footing, we also present our calculations without such a convolution and use the unconvoluted FBA and 3C values of Ref. [13] (see Figure 5 therein). While all theoretical FDCSs in Figure 3 have a common two-peak structure with a larger, binary, peak and a smaller, recoil, peak, they differ in the recoil/binary ratio and in the peaks' positions. On the whole our CQS result provides a ratio which is in better agreement with experiment than in the case of the other theoretical calculations. At the same time, for the binary-peak position we get practically the same discrepancy of almost  $10^\circ$  as obtained with the 3C and WP-CCC approaches. It should be noted that the convolution with experimental uncertainties can explain only about  $2^\circ$  of the discrepancy (see Figure 9 of Ref. [2] and the relevant discussion therein). The unexplained shift suggests therefore that the discussed theoretical treatments may miss some important feature of the binary-encounter mechanism.

#### 4. Summary and Conclusions

We have suggested and applied a novel method for calculating fully differential cross sections for the proton-impact ionization of helium by representing the transition amplitude in terms of amplitudes of the quasi-Sturmian basis functions in parabolic coordinates. The coefficients of the expansion, in the framework of the frozen-core model, are found by solving a driven equation for the three-body system  $(e^-, \text{He}^+, p^+)$ . Specifically, the inhomogeneous matrix equation is obtained by using Sturmian-expansion representations of the Green's function operator  $\hat{G}_0^{(+)}$  and the interaction  $\hat{U}$ , which includes the proton-electron potential, treated as a perturbation. This approach turns out to be effective in the high-energy limit: the convergence of the cross section is achieved with a moderate

number of expansion terms and also at a reasonable size of the matrix representation of the  $p - e$  potential.

The nature of the calculated angular distribution of ejected electrons is common to all theoretical methods. They differ in the ratio of the binary and recoil peak intensities; our CQS approach seems to provide a ratio that is in slightly better agreement with experimental data. In spite of the variety of theoretical approaches, none of them can reproduce the experimentally observed angular position of the binary peak (the discrepancy reaches  $10^\circ$ ). This demands of theory the development of more accurate methods and approaches. For instance, it has been found in [9] that the calculated cross sections, at least at moderate incident energies, are very sensitive to the details on the description of the interaction between the projectile and the target core. We plan to investigate the effect of this short-range part of the projectile–target interaction in the high-energy regime. In addition, we intend to study proton and antiproton impact ionization of heavier atoms, still treated as one-electron targets.

**Author Contributions:** S.A.Z. performed analytical calculations and prepared the original draft. A.S.Z., V.V.N. and D.S.Z. performed analytical and numerical calculations and prepared the figures. L.U.A. performed analytical calculations, discussed results and edited the manuscript. K.A.K. performed analytical calculations and discussed results. All authors have read and agreed to the published version of the manuscript.

**Funding:** This work is supported by the Ministry of Science and Higher Education of the Russian Federation (project no. 0818-2020-0005). The research is carried out using the equipment of the Shared Facility Center “Data Center of FEB RAS” (Khabarovsk, Russia) [26].

**Acknowledgments:** The research was carried out using the equipment of the Shared Facility Center “Data Center of FEB RAS” (Khabarovsk, Russia) [26].

**Conflicts of Interest:** The authors declare no conflict of interest.

## Abbreviations

The following abbreviations are used in this manuscript:

FDCS	fully differential cross section
3C	three Coulomb functions model
CDW-EIS	continuum distorted-wave eikonal initial state model
WP-CCC	wave-packet convergent close-coupling method
CQS	convoluted quasi-Sturmian

## References

- Gassert, H.; Chuluunbaatar, O.; Waitz, M.; Trinter, F.; Kim, H.-K.; Bauer, T.; Laucke, A.; Müller, C.; Voigtsberger, J.; Weller, M.; et al. Agreement of Experiment and Theory on the Single Ionization of Helium by Fast Proton Impact. *Phys. Rev. Lett.* **2016**, *116*, 073201. [[CrossRef](#)] [[PubMed](#)]
- Chuluunbaatar, O.; Kouzakov, K.A.; Zaytsev, S.A.; Zaytsev, A.S.; Shablov, V.L.; Popov, Y.V.; Gassert, H.; Waitz, M.; Kim, H.-K.; Bauer, T.; et al. Single ionization of helium by fast proton impact in different kinematical regimes. *Phys. Rev. A* **2019**, *99*, 062711. [[CrossRef](#)]
- Dörner, R.; Mergel, V.; Jagutzki, O.; Spielberger, L.; Ullrich, J.; Moshhammer, R.; Schmidt-Böcking, H. Cold Target Recoil Ion Momentum Spectroscopy: A ‘momentum microscope’ to view atomic collision dynamics. *Phys. Rep.* **2000**, *330*, 95–192. [[CrossRef](#)]
- Ullrich, J.; Moshhammer, R.; Dorn, A.; Dörner, R.; Schmidt, L.P.H.; Schmidt-Böcking, H. Recoil-ion and electron momentum spectroscopy: Reaction-microscope. *Rep. Prog. Phys.* **2003**, *66*, 1463. [[CrossRef](#)]
- Ullrich, J.; Moshhammer, R.; Dörner, R.; Jagutzki, O.; Mergel, V.; Schmidt-Böcking, H.; Spielberger, L. Recoil-ion momentum spectroscopy. *J. Phys. B* **1997**, *30*, 2917. [[CrossRef](#)]
- Belkic, D.; Gayet, R.; Salin, A. Electron capture in high-energy ion-atom collisions. *Phys. Rep.* **1979**, *56*, 279–369. [[CrossRef](#)]
- Crothers, D.S.F.; Dube, L.J. Continuum Distorted Wave Methods in Ion—Atom Collisions. *Adv. At. Mol. Opt. Phys.* **1992**, *30*, 287–337.
- Voitkiv, A.B. Single ionization of helium by 1-MeV protons. *Phys. Rev. A* **2017**, *95*, 032708. [[CrossRef](#)]
- Igarashi, A.; Gulyás, L. Effective fully differential cross-section in single ionization of helium by fast ions. *J. Phys. B At. Mol. Opt. Phys.* **2019**, *52*, 245203. [[CrossRef](#)]
- Amiri Bidvari, S.; Fathi, R. Applying a four-body continuum-distorted-wave formalism in calculating the fully differential cross section for single ionization of helium in collision with high-energy protons. *Eur. Phys. J. Plus* **2021**, *136*, 190. [[CrossRef](#)]

11. Abdurakhmanov, I.B.; Kadyrov, A.S.; Bray, I.; Bartschat, K. Wave-packet continuum-discretization approach to single ionization of helium by antiprotons and energetic protons. *Phys. Rev. A* **2017**, *96*, 022702. [[CrossRef](#)]
12. Abdurakhmanov, I.B.; Kadyrov, A.S.; Alladustov, S.U.; Bray, I.; Bartschat, K. Fully differential cross sections for single ionization of helium by energetic protons. *Phys. Rev. A* **2019**, *100*, 062708. [[CrossRef](#)]
13. Chuluunbaatar, O.; Zaytsev, S.A.; Kouzakov, K.A.; Galstyan, A.; Shablov, V.L.; Popov, Y.V. Fully differential cross sections for singly ionizing 1-MeV p+He collisions at small momentum transfer: Beyond the first Born approximation. *Phys. Rev. A* **2017**, *96*, 042716. [[CrossRef](#)]
14. Garibotti, C.R.; Miraglia, J.E. Ionization and electron capture to the continuum in the  $H^+$ -hydrogen-atom collision. *Phys. Rev. A* **1980**, *21*, 572–580. [[CrossRef](#)]
15. Brauner, M.; Briggs, J.S.; Klar, J.S. Triply-differential cross sections for ionisation of hydrogen atoms by electrons and positrons. *J. Phys. B* **1989**, *22*, 2265. [[CrossRef](#)]
16. Zaytsev, A.S.; Zaytseva, D.S.; Ancarani, L.U.; Zaytsev, S.A.; Kouzakov, K.A. School of Fundamental and Computer Sciences, Pacific National University, Khabarovsk, Russia. 2022, *to be submitted*.
17. Merkuriev, S.P.; Faddeev, L.D. *Quantum Scattering Theory for Several Particle Systems*, 1st ed.; Springer: Dordrecht, The Netherlands, 1993.
18. Messiah, A. *Quantum Mechanics*; John Wiley & Sons: New York, NY, USA, 1966; Volume 2.
19. Zaytsev, S.A.; Ancarani, L.U.; Zaytsev, A.S.; Kouzakov, K.A. A parabolic quasi-Sturmian approach to quantum scattering by a Coulomb-like potential. *Eur. Phys. J. Plus* **2020**, *135*, 655. [[CrossRef](#)]
20. Abramowitz, M.; Stegun, I.A. (Eds.) *Handbook of Mathematical Functions with Formulas, Graphs, and Mathematical Tables*, 9th ed.; Dover: New York, NY, USA, 1972.
21. Baz, A.; Zeldovich, Y.; Perelomov, A. *Scattering, Reactions, and Decays, in Nonrelativistic Quantum Mechanics*; Nauka: Moscow, Russia, 1966. (In Russian)
22. Shakeshaft, R. Integral representation of the Coulomb Green function derived from the Sturmian expansion. *Phys. Rev. A* **2004**, *70*, 042704. [[CrossRef](#)]
23. Zaytsev, A.S.; Ancarani, L.U.; Zaytsev, S.A. Quasi Sturmian basis for the two-electron continuum. *Eur. Phys. J. Plus* **2016**, *131*, 48. [[CrossRef](#)]
24. Zaytsev, A.S.; Zaytseva, D.S.; Ancarani, L.U.; Zaytsev, S.A. Double ionization of helium with a convoluted quasi Sturmian approach. *Eur. Phys. J. D* **2019**, *73*, 111. [[CrossRef](#)]
25. Chuluunbaatar, O.; Puzynin, I.V.; Vinitsky, P.S.; Popov, Y.V.; Kouzakov, K.A.; Cappello, C.D. Role of the cusp conditions in electron-helium double ionization. *Phys. Rev. A* **2006**, *74*, 014703. [[CrossRef](#)]
26. Sorokin, A.A.; Makogonov, S.V.; Korolev, S.P. The Information Infrastructure for Collective Scientific Work in the Far East of Russia. *Sci. Tech. Inf. Process.* **2017**, *44*, 302–304. [[CrossRef](#)]